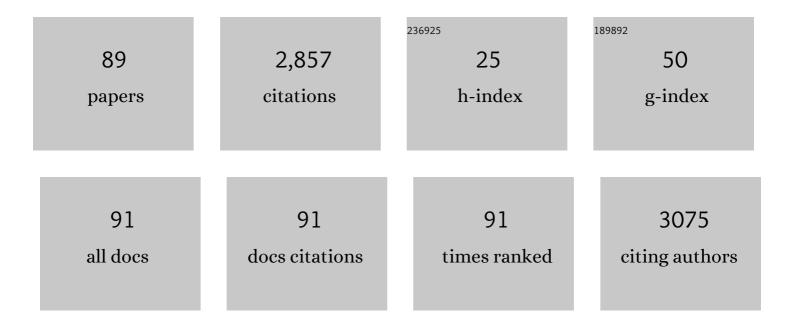
List of Publications by Year in descending order

Source: https://exaly.com/author-pdf/5234268/publications.pdf Version: 2024-02-01



#	Article	IF	CITATIONS
1	A long in situ section of the lower ocean crust: results of ODP Leg 176 drilling at the Southwest Indian Ridge. Earth and Planetary Science Letters, 2000, 179, 31-51.	4.4	456
2	Lithium isotopes in global mid-ocean ridge basalts. Geochimica Et Cosmochimica Acta, 2008, 72, 1626-1637.	3.9	189
3	Strontium isotope evidence for landscape use by early hominins. Nature, 2011, 474, 76-78.	27.8	175
4	The effects of variable sources, processes and contaminants on the composition of northern EPR MORB (8–10°N and 12–14°N): Evidence from volatiles (H2O, CO2, S) and halogens (F, Cl). Earth and Planetary Science Letters, 2006, 251, 209-231.	4.4	151
5	Mantle heterogeneity beneath the southern Mid-Atlantic Ridge: trace element evidence for contamination of ambient asthenospheric mantle. Earth and Planetary Science Letters, 2002, 203, 479-498.	4.4	112
6	Strontium isotope ratios (⁸⁷ Sr/ ⁸⁶ Sr) of tooth enamel: a comparison of solution and laser ablation multicollector inductively coupled plasma mass spectrometry methods. Rapid Communications in Mass Spectrometry, 2008, 22, 3187-3194.	1.5	110
7	Strontium isotope investigation of ungulate movement patterns on the Pleistocene Paleo-Agulhas Plain of the Greater Cape Floristic Region, South Africa. Quaternary Science Reviews, 2016, 141, 65-84.	3.0	82
8	In situ, multiple-multiplier, laser ablation ICP-MS measurement of boron isotopic composition (δ11B) at the nanogram level. Chemical Geology, 2004, 203, 123-138.	3.3	76
9	The oxygen isotope composition of Karoo and Etendeka picrites: High \hat{l} (180 mantle or crustal contamination?. Contributions To Mineralogy and Petrology, 2015, 170, 1.	3.1	73
10	Paleolithic to Bronze Age Siberians Reveal Connections with First Americans and across Eurasia. Cell, 2020, 181, 1232-1245.e20.	28.9	71
11	Light Stable Isotopic Compositions of Enriched Mantle Sources: Resolving the Dehydration Paradox. Geochemistry, Geophysics, Geosystems, 2017, 18, 3801-3839.	2.5	70
12	Strontium isotope ratios in fossil teeth from South Africa: assessing laser ablation MC-ICP-MS analysis and the extent of diagenesis. Journal of Archaeological Science, 2010, 37, 1437-1446.	2.4	65
13	Peridotitic Lithosphere Metasomatized by Volatile-bearing Melts, and its Association with Intraplate Alkaline HIMU-like Magmatism. Journal of Petrology, 2016, 57, 2053-2078.	2.8	56
14	Origin and evolution of the â^¼1.9 Ga Richtersveld Magmatic Arc, SW Africa. Precambrian Research, 2017, 292, 417-451.	2.7	53
15	Earliest Evidence for the Ivory Trade in Southern Africa: Isotopic and ZooMS Analysis of Seventh–Tenth Century ad Ivory from KwaZulu-Natal. African Archaeological Review, 2016, 33, 411-435.	1.4	51
16	Geochemical and isotopic constraints on the tectonic and crustal evolution of the Shackleton Range, East Antarctica, and correlation with other Gondwana crustal segments. Precambrian Research, 2010, 180, 85-112.	2.7	49
17	Selenium and tellurium systematics in MORBs from the southern Mid-Atlantic Ridge (47–50°S). Geochimica Et Cosmochimica Acta, 2014, 144, 379-402.	3.9	47
18	Crystallization processes beneath the southern Mid-Atlantic Ridge (40–55°S), evidence for high-pressure initiation of crystallization. Contributions To Mineralogy and Petrology, 2002, 142, 582-602.	3.1	46

#	Article	IF	CITATIONS
19	Magmatic effects of the Cobb hot spot on the Juan de Fuca Ridge. Journal of Geophysical Research, 2005, 110, .	3.3	45
20	MORB melting processes beneath the southern Mid-Atlantic Ridge (40–55°S): a role for mantle plume-derived pyroxenite. Contributions To Mineralogy and Petrology, 2002, 144, 206-229.	3.1	40
21	Implications of the distribution, age and origins of the granites of the Mesoproterozoic Spektakel Suite for the timing of the Namaqua Orogeny in the Bushmanland Subprovince of the Namaqua-Natal Metamorphic Province, South Africa. Precambrian Research, 2018, 312, 68-98.	2.7	40
22	Strontium isotope analyses of large herbivore habitat use in the Cape Fynbos region of South Africa. Oecologia, 2010, 164, 567-578.	2.0	39
23	Diffusion-zoned pyroxenes in an isotopically heterogeneous mantle lithosphere beneath the Dunedin Volcanic Group, New Zealand, and their implications for intraplate alkaline magma sources. Lithosphere, 2017, 9, 463-475.	1.4	30
24	Lithium isotope analysis of natural and synthetic glass by laser ablation MC-ICP-MS. Journal of Analytical Atomic Spectrometry, 2010, 25, 1033.	3.0	29
25	The Anita Peridotite, New Zealand: Ultra-depletion and Subtle Enrichment in Sub-arc Mantle. Journal of Petrology, 2016, 57, 717-750.	2.8	28
26	Sr- and Nd- isotope variations along the Pleistocene San Pedro – Linzor volcanic chain, N. Chile: Tracking the influence of the upper crustal Altiplano-Puna Magma Body. Journal of Volcanology and Geothermal Research, 2017, 341, 172-186.	2.1	27
27	Strontium isotope analysis of curved tooth enamel surfaces by laser-ablation multi-collector ICP-MS. Palaeogeography, Palaeoclimatology, Palaeoecology, 2014, 416, 142-149.	2.3	26
28	In Situ 87Sr/86Sr of Scheelite and Calcite Reveals Proximal and Distal Fluid-Rock Interaction During Orogenic W-Au Mineralization, Otago Schist, New Zealand. Economic Geology, 2018, 113, 1571-1586.	3.8	26
29	Magmatic differentiation at La Poruña scoria cone, Central Andes, northern Chile: Evidence for assimilation during turbulent ascent processes, and genetic links with mafic eruptions at adjacent San Pedro volcano. Lithos, 2019, 338-339, 128-140.	1.4	24
30	The Dunedin Volcanic Group and a revised model for Zealandia's alkaline intraplate volcanism. New Zealand Journal of Geology, and Geophysics, 2020, 63, 510-529.	1.8	24
31	Linking the mafic volcanism with the magmatic stages during the last 1â€ ⁻ Ma in the main volcanic arc of the Altiplano-Puna Volcanic Complex (Central Andes). Journal of South American Earth Sciences, 2019, 95, 102295.	1.4	23
32	The Keimoes Suite redefined: The geochronological and geochemical characteristics of the ferroan granites of the eastern Namaqua Sector, Mesoproterozoic Namaqua-Natal Metamorphic Province, southern Africa. Journal of African Earth Sciences, 2017, 134, 737-765.	2.0	22
33	Late Neolithic-Chalcolithic socio-economical dynamics in Northern Iberia. A multi-isotope study on diet and provenance from Santimamiñe and Pico Ramos archaeological sites (Basque Country, Spain). Quaternary International, 2018, 481, 14-27.	1.5	21
34	The upper crustal magma plumbing system of the Pleistocene Apacheta-Aguilucho Volcanic Complex area (Altiplano-Puna, northern Chile) as inferred from the erupted lavas and their enclaves. Journal of Volcanology and Geothermal Research, 2019, 373, 179-198.	2.1	21
35	Multi-isotopic and morphometric evidence for the migration of farmers leading up to the Inka conquest of the southern Andes. Scientific Reports, 2020, 10, 21171.	3.3	19
36	Multiâ€ŧissue and multiâ€ɨsotope (ĺ´ ¹³ C, ĺ´ ¹⁵ N, ĺ´ ¹⁸ O and) Tj ETQqO O eO3349.	O rgBT /Ove 3.2	erlock 10 Tf 50 17

3

#	Article	IF	CITATIONS
37	Territorial mobility and subsistence strategies during the Ebro Basin Late Neolithic-Chalcolithic: A multi-isotope approach from San Juan cave (Loarre, Spain). Quaternary International, 2018, 481, 28-41.	1.5	16
38	Low-l´180 zircon xenocrysts in alkaline basalts; a window into the complex carbonatite-metasomatic history of the Zealandia lithospheric mantle. Geochimica Et Cosmochimica Acta, 2019, 254, 21-39.	3.9	16
39	Petrological, geochemical and isotopic data of Neoproterozoic rock units from Uruguay and South Africa: Correlation of basement terranes across the South Atlantic. Gondwana Research, 2020, 80, 12-32.	6.0	16
40	Environmental and ecological implications of strontium isotope ratios in mid-Pleistocene fossil teeth from Elandsfontein, South Africa. Palaeogeography, Palaeoclimatology, Palaeoecology, 2018, 490, 84-94.	2.3	15
41	Dating agpaitic rocks: A multi-system (U/Pb, Sm/Nd, Rb/Sr and 40Ar/39Ar) isotopic study of layered nepheline syenites from the IlĀmaussaq complex, Greenland. Lithos, 2019, 324-325, 74-88.	1.4	15
42	Petrogenesis of peralkaline granite dykes of the Straumsvola complex, western Dronning Maud Land, Antarctica. Contributions To Mineralogy and Petrology, 2018, 173, 1.	3.1	14
43	Geological evolution of Paniri volcano, Central Andes, northern Chile. Journal of South American Earth Sciences, 2018, 84, 184-200.	1.4	14
44	Constraining the sub-arc, parental magma composition for the giant Altiplano-Puna Volcanic Complex, northern Chile. Scientific Reports, 2020, 10, 6864.	3.3	14
45	Sunda arc mantle source l´180 value revealed by intracrystal isotope analysis. Nature Communications, 2021, 12, 3930.	12.8	14
46	Crustal versus mantle origin of carbonate xenoliths from Kimberley region kimberlites using C-O-Sr-Nd-Pb isotopes and trace element abundances. Geochimica Et Cosmochimica Acta, 2019, 266, 258-273.	3.9	13
47	Re-evaluating Scythian lifeways: Isotopic analysis of diet and mobility in Iron Age Ukraine. PLoS ONE, 2021, 16, e0245996.	2.5	13
48	Element and Sr–O isotope redistribution across a plate boundary-scale crustal serpentinite mélange shear zone, and implications for the slab-mantle interface. Earth and Planetary Science Letters, 2019, 522, 198-209.	4.4	12
49	The geochemistry and geochronology of the upper granulite facies Kliprand dome: Comparison of the southern and northern parts of the Bushmanland Domain of the Namaqua Metamorphic Province, southern Africa and clues to its evolution. Precambrian Research, 2019, 330, 58-100.	2.7	12
50	Petrogenesis of the diamondiferous Pipe-8 ultramafic intrusion from the Wajrakarur kimberlite field of Southern India and its relation to the worldwide Mesoproterozoic (~1.1Â Ga) magmatism of kimberlite and related rocks. Geoscience Frontiers, 2020, 11, 793-805.	8.4	12
51	Natural Clinopyroxene Reference Materials for in situ Sr Isotopic Analysis via LA-MC-ICP-MS. Frontiers in Chemistry, 2020, 8, 594316.	3.6	12
52	The great escape: Petrogenesis of low-silica volcanism of Pliocene to Quaternary age associated with the Altiplano-Puna Volcanic Complex of northern Chile (21°10′-22°50′S). Lithos, 2019, 346-347, 105162	. ^{1.4}	11
53	The ups & downs of Iron Age animal management on the Oxfordshire Ridgeway, south-central England: A multi-isotope approach. Journal of Archaeological Science, 2019, 101, 199-212.	2.4	11
54	From texts to teeth: A multi-isotope study of sheep and goat herding practices in the Late Bronze Age (â€~Mycenaean') polity of Knossos, Crete. Journal of Archaeological Science: Reports, 2019, 23, 36-56.	0.5	10

#	Article	IF	CITATIONS
55	Spatial variation in bioavailable strontium isotope ratios (87Sr/86Sr) in Kenya and northern Tanzania: Implications for ecology, paleoanthropology, and archaeology. Palaeogeography, Palaeoclimatology, Palaeoecology, 2020, 560, 109957.	2.3	10
56	Geology, geochemistry and Sr–Nd constraints of selected metavolcanic rocks from the eastern boundary of the Saharan Metacraton, southern Sudan: A possible revision of the eastern boundary. Precambrian Research, 2016, 281, 566-584.	2.7	9
57	The 1.8ÂGa Gladkop Suite: The youngest Palaeoproterozoic domain in the Namaqua-Natal Metamorphic Province, South Africa. Precambrian Research, 2020, 350, 105941.	2.7	9
58	The geology and geochemistry of the Espungabera Formation of central Mozambique and its tectonic setting on the eastern margin of the Kalahari Craton. Journal of African Earth Sciences, 2015, 101, 96-112.	2.0	8
59	Enamel isotopic data from the domesticated animals at Kotada Bhadli, Gujarat, reveals specialized animal husbandry during the Indus Civilization. Journal of Archaeological Science: Reports, 2018, 21, 183-199.	0.5	8
60	Heading for the hills? A multi-isotope study of sheep management in first-millennium BC Italy. Journal of Archaeological Science: Reports, 2020, 29, 102036.	0.5	8
61	The role of crustal contamination in the petrogenesis of nepheline syenite to granite magmas in the Ditrău Complex, Romania: evidence from O-, Nd-, Sr- and Pb-isotopes. Contributions To Mineralogy and Petrology, 2020, 175, 1.	3.1	8
62	Eruptive history of La Poruña scoria cone, Central Andes, Northern Chile. Bulletin of Volcanology, 2020, 82, 1.	3.0	8
63	Peritectic assemblage entrainment as the main compositional driver in the I-type Vredenburg Granite, north-western Pan-African Saldania Belt, South Africa: A whole-rock chemical perspective. Lithos, 2020, 364-365, 105522.	1.4	8
64	Intraplate volcanism on the Zealandia Eocene-Early Oligocene continental shelf: the Waiareka-Deborah Volcanic Field, North Otago. New Zealand Journal of Geology, and Geophysics, 2020, 63, 450-468.	1.8	7
65	Saline groundwater in the Buffels River catchment, Namaqualand, South Africa: A new look at an old problem. Science of the Total Environment, 2021, 762, 143140.	8.0	7
66	Human mobility at Tell Atchana (Alalakh), Hatay, Turkey during the 2nd millennium BC: Integration of isotopic and genomic evidence. PLoS ONE, 2021, 16, e0241883.	2.5	7
67	Petrogenesis of lamprophyres synchronous to kimberlites from the Wajrakarur kimberlite field: Implications for contrasting lithospheric mantle sources and geodynamic evolution of the eastern Dharwar Craton of southern India. Geological Journal, 2019, 54, 2994-3016.	1.3	6
68	The life-history of a late Mesolithic woman in Iberia: A sequential multi-isotope approach. Quaternary International, 2020, 566-567, 233-244.	1.5	6
69	Pyrometamorphosed Otago Schist xenoliths cause minor contamination of Dunedin Volcanic Group basanite. New Zealand Journal of Geology, and Geophysics, 2020, 63, 530-546.	1.8	6
70	The geology and geochemistry of the Straumsnutane Formation, Straumsnutane, western Dronning Maud Land, Antarctica and its tectonic setting on the western margin of the Kalahari Craton: additional evidence linking it to the Umkondo Large Igneous Province. Geological Society Special Publication, 2017, 457, 61-85.	1.3	5
71	Anthropic resource exploitation and use of the territory at the onset of social complexity in the Neolithic-Chalcolithic Western Pyrenees: a multi-isotope approach. Archaeological and Anthropological Sciences, 2019, 11, 3665-3680.	1.8	5
72	The Mount Cameroon southwest flank eruptions: Geochemical constraints on the subsurface magma plumbing system. Journal of Volcanology and Geothermal Research, 2019, 384, 179-188.	2.1	5

#	Article	IF	CITATIONS
73	Upper crustal differentiation processes and their role in 238U-230Th disequilibria at the San Pedro-Linzor volcanic chain (Central Andes). Journal of South American Earth Sciences, 2020, 102, 102672.	1.4	5
74	Evolution of the Azufre volcano (northern Chile): Implications for the Cerro Pabellón Geothermal Field as inferred from long lasting eruptive activity. Journal of Volcanology and Geothermal Research, 2022, 423, 107472.	2.1	5
75	Petrogenesis of amphibole megacrysts in lamprophyric intraplate magmatism in southern New Zealand. New Zealand Journal of Geology, and Geophysics, 2020, 63, 489-509.	1.8	4
76	Interdisciplinary Analysis of the Lehi Horse: Implications for Early Historic Horse Cultures of the North American West. American Antiquity, 0, , 1-21.	1.1	4
77	Bioavailable Strontium, Human Paleogeography, and Migrations in the Southern Andes: A Machine Learning and GIS Approach. Frontiers in Ecology and Evolution, 2021, 9, .	2.2	4
78	Physical and chemical evolution of the largest monogenetic lava field in the Central Andes: El Negrillar Volcanic Field, Chile. Journal of Volcanology and Geothermal Research, 2022, 426, 107541.	2.1	4
79	Distinct scheelite REE geochemistry and 87Sr/86Sr isotopes in proximally- and distally-sourced metamorphogenic hydrothermal systems, Otago Schist, New Zealand. Ore Geology Reviews, 2022, 144, 104800.	2.7	4
80	Human mobility in Byzantine Cyprus: A case study from the Hill of Agios Georgios, Nicosia. Quaternary International, 2021, , .	1.5	4
81	Investigating Cattle Procurement at Great Zimbabwe Using 87Sr/86Sr. Journal of African Archaeology, 2021, 19, 146-158.	0.6	3
82	The genesis and age of the Grunehogna Granite and Rb–Sr and Sm–Nd chemistry of the Annandagstoppane Granite, Ahlmanryggen, Dronning Maud Land, Antarctica. Polar Science, 2021, 30, 100717.	1.2	3
83	The role of ostrich in shaping the landscape use patterns of humans and hyenas on the southern coast of South Africa during the late Pleistocene. , 2018, , 333-346.		3
84	Population movements of the Huron-Wendat viewed through strontium isotope analysis. Journal of Archaeological Science: Reports, 2020, 33, 102466.	0.5	2
85	Sea, sickness and cautionary tales: a multi-isotope study from a post-mediaeval hospital at the city-port of Gibraltar (AD 1462–1704). Archaeological and Anthropological Sciences, 2020, 12, 1.	1.8	2
86	Scale of human mobility in northwestern Patagonia: An approach based on regional geology and strontium isotopes in human remains. Geoarchaeology - an International Journal, 2022, 37, 227-241.	1.5	2
87	An investigation into the 87Sr/86Sr radiogenic isotope geochemistry of the manganese ore of the Kalahari Manganese Field with a view on hydrothermal fluid flow and related rare earth element enrichments. South African Journal of Geology, 2019, 122, 237-248.	1.2	1
88	Lead and strontium isotopes as palaeodietary indicators in the Western Cape of South Africa. South African Journal of Science, 2020, 116, .	0.7	1
89	Structural Controls on Shallow Cenozoic Fluid Flow in the Otago Schist, New Zealand. Geofluids, 2020, 2020, 1-25.	0.7	1